CLM-P157

CLM-P157

United Kingdom Atomic Energy Authority

RESEARCH GROUP

Preprint

THE ION CYCLOTRON DRIFT LOSS-CONE INSTABILITY IN MIRROR MAGNETIC WELLS

J. G. CORDEY
L. G. KUO-PETRAVIC
M. PETRAVIC

Culham Laboratory
Abingdon Berkshire

1967

UNCLASSIFIED
(Approved for Publication)

CLM - P 157

THE ION CYCLOTRON DRIFT LOSS-CONE INSTABILITY IN MIRROR MAGNETIC WELLS

by

J.G. CORDEY
L.G. KUO-PETRAVIC
M. PETRAVIC

(Submitted for publication in Nuclear Fusion)

A B S T R A C T

The ion cyclotron drift loss-cone instability is studied for the case of steep particle density gradients $(\frac{1}{n}\frac{dn}{dr}a_i \simeq -0{\cdot}3)$, magnetic field gradients and finite plasma dimensions. Computational results show that there are no high density stable regimes. It is found that for a mirror velocity distribution the magnetic well field gradient is destabilizing, in contrast to the stabilizing effect found by Krall and Fowler for a near-Maxwellian velocity distribution. Potential distributions and critical densities are found for a slab model using appropriate boundary conditions to determine the modes. The threshold densities for the boundary value case are only slightly higher than that given by the usual local approximation. Frequencies and growth rates as functions of azimuthal wave number are found for the instability for typical PHOENIX II and ALICE parameters.

U.K.A.E.A. Research Group,
Culham Laboratory,
Abingdon,
Berks.

December, 1967 (ED)

C O N T E N T S

1. INTRODUCTION

The ion cyclotron drift instability[1] is a result of the non-Maxwellian ion velocity distribution. In toroidal systems this is due to the pressure gradient, and in magnetic mirrors it is mostly due to the presence of a loss-cone. Since the deviations from the Maxwellian distribution are larger in mirror experiments than toroidal ones, the instability can be expected to have larger growth rates in mirror confined plasmas. The density threshold for this instability may be estimated by realising that the wave which couples to the gyro-frequency Ω_i is here the electron drift wave with frequency $\omega = \frac{\omega_{pi}^2}{\Omega_i} \frac{\varepsilon}{k_y}$ where ω_{pi} is the ion plasma frequency, ε^{-1} the density gradient scale length and k_y the wave number. The coupling condition $\omega = \Omega_i$ therefore requires that $\omega_{pi} \geqslant \Omega_i$.

The ion cyclotron drift instability was first discussed by Mikhailovskii and Timofeev[1] in 1963, for near-Maxwellian plasmas. It was shown by Post and Rosenbluth[2] in 1966 to be a serious instability for loss-cone types of plasmas; density gradients lower than $\varepsilon a_i = \frac{1}{n_o} \frac{dn_o}{dr} a_i \simeq 0{\cdot}01$ where a_i is the mean ion gyro-radius, were required to obtain stability at densities of about 10^{13} cm^{-3}. It would be difficult to employ such low gradients in a fusion reactor and in most existing experiments they are larger. Thus it is worth while searching for even moderate stabilising effects. By numerical methods we have been able to ascertain quantitatively the stability boundaries, frequencies, growth rates, and wavelengths of this instability for present day mirror machines like PHOENIX II and Alice.

Following the work of Post and Rosenbluth[2], Post[3] has investigated the stability of a loss cone type distribution and concluded

that for sufficiently large plasma density gradients there existed a stable region at high plasma densities. Since quite large density gradients, e.g. $\varepsilon a_i \approx -0{\cdot}3$, are present in some experiments, we have examined this case (Section 2) in more detail and included terms which were omitted in the analysis of the above authors.

In Section 3 we examine, using the local approximation, the effect upon the instability of magnetic field inhomogeneity. Since in magnetic well confinement, there is always present a magnetic field gradient $\frac{1}{B}\frac{dB}{dr}$ of opposing sign to the density gradient $\frac{1}{n_o}\frac{dn_o}{dr}$, it is interesting to consider its effect on the stability boundary and frequency. Krall and Fowler[4] have recently shown that a cusp-like magnetic field curvature can stabilise completely a locally Maxwellian plasma. However the effect of the field curvature on a loss-cone distribution is more complex. The electron drift wave frequency is enhanced by a factor

$$\left(1 - \frac{2\frac{1}{B}\frac{dB}{dr}}{\frac{1}{n}\frac{dn}{dr}}\right)$$

which originates from the fact that,

$$\operatorname{div} \bar{v}' = \operatorname{div} \frac{\vec{E} \times \vec{B}}{B^2} \neq 0$$

in a nonuniform magnetic field, this increases the magnitude of the term proportional to $\omega \frac{\partial f_o}{\partial v_\perp^2}$ which for a locally Maxwellian plasma leads to stabilisation; however for a loss-cone type of distribution this term is destabilising. This is shown both analytically and by computation in Section 3.

Finally in Section 4, we abandon the local approximation and attempt to take into account the finite size of plasma. Shima and Fowler[5] first treated this problem in cylindrical geometry and

found that, under certain conditions, the radial potential variation may be approximated by a Bessel function. Here, we examine the critical density for an arbitrary loss-cone distribution as a function of the radial wave number in a plasma slab with appropriate boundary conditions. The results show that the instability in a plasma slab with a linear density gradient has a growth rate only slightly less than that predicted by the local approximation for the point of maximum density in the slab.

2. HIGH ION DENSITY GRADIENT

In order to facilitate a close comparison of our results with that of Post and Rosenbluth[2], we have expressly adopted the same basic premises and used the same ion loss-cone distribution functions. We assume an infinite plasma slab with a linear density gradient in the x-direction and examine the marginal stability curve in the local approximation, that is, at a point $x = 0$. The density gradient at this point is given by $\varepsilon = \frac{1}{n_0}\frac{dn_0}{dx}$ where n_0 is the particle density at $x = 0$. The equilibrium distribution function is necessarily of the form:-

$$f_{0j} = f_0\,(v_\perp^2,\ v_\parallel^2)\left(1 + \varepsilon\left(x + \frac{v_y}{\Omega_j}\right)\right). \qquad \ldots (1)$$

where j denotes the species, ion or electron, and Ω_j the cyclotron frequency.

The normalization is given by:

$$\int_0^\infty \int_{-\infty}^{\infty} \int_0^{2\pi} f_0\, v_\perp\, dv_\perp\, dv_\parallel\, d\psi = 1$$

where the cylindrical co-ordinates $(v_\perp,\ v_\parallel,\ \psi)$ are used.

The perturbed density f_1 is obtained by integration along the particle orbits in the unperturbed magnetic field

$$f_{1j} = \frac{-e\eta_j}{m_j} \int_{-\infty}^{t} \vec{E} \cdot \frac{\partial f_o(v')}{\partial \vec{v}'} \, dt' \qquad \ldots (2)$$

where η_j denotes the sign of the electric charge e. Let us assume that the perturbed potential is of the form

$$\varphi = \exp i(\omega t + k_y y)$$

and

$$E = - \nabla\varphi = - ik_y \varphi \ .$$

To obtain the perturbed distribution one first calculates $\frac{\partial f_{oj}}{\partial v_y'}$ using equation (1)

$$\frac{\partial f_{oj}}{\partial v_y'} = \frac{\varepsilon}{\Omega_j} f_o(v_\perp^2, v_\parallel^2) + \left(1 + \varepsilon(x + \frac{v_y}{\Omega_j}) \right) 2v_y' \frac{\partial f_o(v_\perp^2, v_\parallel^2)}{\partial v_\perp^2}$$

Inserting the result into equation (2), the perturbation becomes

$$f_{1ion} = \frac{e\varphi}{m_i} \left\{ 2(1+\varepsilon x) \frac{\partial f_o}{\partial v_\perp^2} - \left[2\omega \ (1+\varepsilon x) \frac{\partial f_o}{\partial v_\perp^2} - \frac{\varepsilon k_y}{\Omega_i} f_o \right] I_1 \right.$$

$$\left. + \frac{2\varepsilon}{\Omega_i} \frac{\partial f_o}{\partial v_\perp^2} \ (v_y - \omega \, v_y \, I_1) \right\}$$

where

$$I_1 = \sum_{n,m=-\infty}^{\infty} \frac{J_n\left(\frac{k_y \, v_\perp}{\Omega_i} \right) J_m\left(\frac{k_y \, v_\perp}{\Omega_i} \right) \exp(i(n-m) \, \psi)}{\omega - n \, \Omega_i}$$

Hence the perturbation in ion density is

$$4\pi \, \rho_i = 4\pi \, n_o e \int f_{1j} \, d^3v$$

$$= - 2\pi \, \omega_{pi}^2 \, \varphi \, (1+\varepsilon x) \, 2\Omega \sum_{n=-\infty}^{\infty} \frac{\int \frac{\partial f_o}{\partial v_\perp^2} J_n^2\left(\frac{k_y v_\perp}{\Omega_i} \right) v_\perp \, dv_\perp \, dv_\parallel}{\Omega + n}$$

$$+ 2\pi \, \omega_{pi}^2 \, \varphi \, \frac{k_y \varepsilon}{\Omega_i^2} \sum_{n=-\infty}^{\infty} \frac{\int f_o J_n^2\left(\frac{k_y \, v_\perp}{\Omega_i} \right) v_\perp \, dv_\perp \, dv_\parallel}{\Omega + n}$$

$$+ 2\pi \, \omega_{pi}^2 \, \varphi \, \frac{\varepsilon}{k_y} \, 2\Omega \sum_{n=-\infty}^{\infty} \frac{\int \frac{\partial f_o}{\partial v_\perp^2} \, n \, J_n^2\left(\frac{k_y \, v_\perp}{\Omega_i} \right) v_\perp \, dv_\perp \, dv_\parallel}{\Omega - n} \qquad \ldots (3)$$

where $\Omega = \frac{\omega}{\Omega_i}$. Here the first term on the right hand side of equation (3) depends on the shape of the velocity distribution, in particular on the positive slope $\frac{\partial f_o}{\partial v_\perp^2}$ of a loss-cone type distribution. The second term is the ion density gradient term omitted in the computations of Ref.(3) because of the assumption $\frac{\varepsilon\, v_\perp^2\, k_y}{\Omega_i\, \omega} \ll 1$. The electron perturbed density is much simplified because of the assumption $\omega \ll |\Omega_e|$ and $k_y\, v_{\perp e} \ll |\Omega_e|$, and is given by

$$4\pi\, \rho_e = -\,(1 + \varepsilon x)\, \frac{\omega_{pe}^2}{\Omega_e^2}\, k_y^2\, \varphi + \omega_{pe}^2\, \frac{k_y\, \varepsilon}{\Omega_e\, \omega}\, \varphi \qquad \ldots (4)$$

The last term on the right hand side of equation (4) is the dominant electron drift term which cancels exactly the ion density gradient term mentioned previously in the limit of low frequencies.

The Poisson's equation then leads to the dispersion equation which can most conveniently be written in the following form

$$\frac{1}{D} = \frac{-m_e}{m_i} + \frac{F_1}{\alpha^2}\left(1 - \frac{\varepsilon a_i}{\alpha}\,\Omega\right) + \left(F_2 - \frac{1}{\Omega}\right)\frac{\varepsilon a_i}{\alpha}$$

$$= G(\Omega,\, k_y,\, \varepsilon) \qquad \ldots (5)$$

where

$$D = \frac{\omega_{pi}^2}{\Omega_i^2}\ ,\quad \alpha = k_y\, a_i\ ,\quad a_i = \frac{\sqrt{\bar{v}^2}}{\Omega_i}$$

and $\sqrt{\bar{v}^2}$ is the root mean square ion velocity given by the velocity distribution function. The functions F_1 and F_2 are defined by

$$F_1 = -\,\Omega^2 \sum_{n=1}^{\infty} \frac{(2n-1)}{(n^2 - \Omega^2)\left((n-1)^2 - \Omega^2\right)}\, I_{n-1,n}\,(\alpha y)$$

with

$$I_{n-1,n}\,(\alpha y) = -\,4\alpha \int_o^{\infty} dy\ \Psi\,(y^2)\ J_{n-1}\,(\alpha y)\ J_n(\alpha y)$$

and

$$F_2 = \frac{K_o}{\Omega} + \sum_{n=1}^{\infty} \frac{2\Omega K_n}{(\Omega^2 - n^2)}$$

with

$$K_o = \int_0^{\infty} dy \; 2y \; \Psi(y^2) \; J_o^2(\alpha y)$$

$$K_n = \int_0^{\infty} dy \; 2y \; \Psi(y^2) \; J_n^2(\alpha y)$$

The change of variables from $v_\perp$ to y was performed according to

$$v_\perp^2 = y^2 \bar{v}^2 \quad , \quad \frac{\Psi(y^2)}{\pi \bar{v}^2} = \int_{-\infty}^{\infty} f_o \, dv_\parallel \quad .$$

In Fig.1 we have plotted the dispersion equation given by equation (33) of Ref.(2) which does not include the ion density gradient term for a mirror ratio of 10 and for $\alpha = 10$ and $\varepsilon a_i = -0{\cdot}8$.

In our notation this equation is of the form

$$\frac{1}{D} = \frac{-m_e}{m_i} + \frac{F_1}{\alpha^2} - \frac{\varepsilon a_i}{\Omega \alpha} = H(\Omega, k_y, \varepsilon) \qquad \ldots (5A)$$

In Fig.2, the dispersion equation (5) which contains the ion density gradient term, is plotted[6]. The roots Ω_n are obtained graphically from the intercepts of the right hand side of the equation plotted in Figs.1 and 2 with the horizontal line H or $G = \frac{1}{D}$. In the stable regions the number of stable roots is equal to the number of harmonics of Ω_i. It may be seen in Fig.1 that, it was possible by making the electron gradient term large enough, to obtain bands of stable regions at high density. However, Fig.2 shows that if all ion terms are included, the upper stable regions do not exist.

To examine in more detail the effect of the ion gradient term on the critical density for the onset of the instability, $\frac{1}{D_{crit}}$ was calculated as a function of $\alpha = k_y a_i$ for a more realistic velocity distribution:- AF′ of Ref.(2) - corresponding to a mirror ratio R of 1·5, with a density gradient $\varepsilon a_i = -0{\cdot}3$. The results, with and without the ion density gradient term differ by about 20% as shown in Fig.3. In both cases, the most unstable wave number is around $\alpha = 2{\cdot}5$, while for $\alpha < 2$, the plasma is stable for all densities.

3. EFFECT OF MAGNETIC FIELD INHOMOGENEITY

In this section we examine the effect upon the instability of the inhomogeneity in the magnetic field again in the local approximation. In a mirror machine, the curvature and transverse inhomogeneity of the magnetic field lead to particle drifts

$$v_c = \frac{v_{\parallel}^2}{R_c\ \Omega_j}$$

and

$$v_t = \frac{v_{\perp}^2}{2\Omega_j}\ \frac{1}{B}\ \frac{dB}{dr} = \frac{v_{\perp}^2}{2R_c\ \Omega_j}$$

respectively, where R_c is the radius of curvature of the magnetic field. The dispersion equation which is derived from equation (2) and the Poisson's equation may be written in the form

$$1 = -\sum_j \frac{2\pi\omega_{pj}^2}{k_y^2} \iint \left\{ 2\ \frac{\partial f_{oj}}{\partial v_{\perp}^2} + (2\omega\ \frac{\partial f_{oj}}{\partial v_{\perp}^2} - \frac{k_y \varepsilon f_{oj}}{\Omega_j}) \sum_n \frac{J_n^2(\frac{k_y v_{\perp}}{\Omega_i})}{\omega - n\Omega + k_y v_{Dj}} \right\} v_{\perp}\ dv_{\perp}\ dv_{\parallel} \qquad \ldots (6)$$

where

$$v_{Dj} = \frac{\frac{1}{2}(v_{\perp}^2 + 2v_{\parallel}^2)}{R_c\ \Omega_j}$$

To simplify the electron terms of the dispersion equation, we assume that the distribution function is Maxwellian,

$$f_{oe} = \frac{\pi^{-3/2}}{v_{\theta e}^3} \; e^{-\frac{v^2}{v_{\theta e}^2}}$$

and take $\left|\frac{k_y \, v_\perp}{\Omega_e}\right| \ll 1$, the electron term then becomes

$$4\pi \, en_e' = -\frac{\omega_{pe}^2 \, k_y^2}{\Omega_e^2} \, \varphi + \frac{\omega_{pe}^2 \, k_y \, (\varepsilon - \frac{2}{R_C})}{\Omega_e \, \omega} \, \varphi \; .$$

Since we want to exhibit both the effects of a hole in the ion distribution at $v_\perp = 0$ caused by the loss-cone, as well as the ion density gradient, we take the velocity distribution for ions in the form

$$f_o(v_\perp, \, v_\parallel) = \frac{\left(\frac{v_\perp}{v_{\perp o}}\right)^{2P}}{\pi^{3/2} \, \Gamma(p+1) \, v_{\perp o}^2 \, v_{\parallel o}} \; e^{-\left(\frac{v_\perp^2}{v_{\perp o}^2} + \frac{v_\parallel^2}{v_{\parallel o}^2}\right)} \qquad \ldots \; (7)$$

To further simplify the ion terms of the dispersion equation, we assume that for the unstable waves $|\omega - n \, \Omega_i| \ll |\omega - (n \pm 1) \, \Omega_i|$ and consider only one ion term. With the above approximations, the dispersion relation equation (6) becomes

$$1 = \frac{-\omega_{pe}^2}{\Omega_e^2} + \frac{\omega_{pe}^2 \, (\varepsilon - \frac{2}{R_C})}{k_y \, \Omega_e \, \omega}$$

$$- \frac{\omega_{pi}^2}{\pi^{1/2} \, k_y^2 \, v_{\perp o}^2 \, v_{\parallel o} \, \Gamma \, (p+1)} \iint \left\{ 2\omega \, (p - u_\perp^2) - \frac{k_y \, \varepsilon \, v_{\perp o}^2 u_\perp^2}{\Omega_i} \right\}$$

$$\frac{J_n^2 \, (\alpha^* \, u_\perp)}{\omega - n \, \Omega_i + k_y \, v_{Di}} \; u_\perp^{2(p-1)} \; e^{-(u_\perp^2 + u_\parallel^2)} \; u_\perp \, du_\perp \, du_\parallel \qquad \ldots \; (8)$$

where

$$u_\perp = \frac{v_\perp}{v_{\perp o}} \quad , \quad u_\parallel = \frac{v_\parallel}{v_{\parallel o}} \quad , \quad \text{and} \quad \alpha^* = \frac{k_y \, v_{\perp o}}{\Omega_i}$$

Using the same procedure as Krall and Fowler[4] to simplify the integration over $u_\perp$ and $u_\parallel$, the denominator of the ion terms was expanded in the form

$$\frac{1}{\omega - n\,\Omega_i + k_y\,v_{Di}} \approx \frac{1}{(\omega - n\,\Omega_i)}\left\{\,1 - \frac{k_y\,v_{Di}}{\omega - n\,\Omega_i} + \cdots\,\right\} .$$

This procedure is valid provided $|\omega - n\,\Omega_i| \gg k_y\,v_{Di}$. Summing the integrated series the dispersion equation may be written in the form

$$1 + \frac{\omega_{pe}^2}{\Omega_e^2} = \frac{\omega_{pe}^2\,(\varepsilon - \frac{2}{R_C})}{k_y\,\Omega_e\,\omega} - \frac{\omega_{pi}^2}{k_y^2\,v_{\perp o}^2}\,\frac{2\omega A - \alpha^*\,\varepsilon a_i^*\,\Omega_i\,B}{\omega - n\,\Omega_i + k_y\,\bar{v}_{Di}} \qquad \ldots (9)$$

where

$$A = \frac{1}{\Gamma(p+1)}\int (p - u_\perp^2)\,J_n^2(\alpha^*\,u_\perp)\,u_\perp^{2(p-1)}\,e^{-u_\perp^2}\,u_\perp\,du_\perp$$

$$B = \frac{1}{\Gamma(p+1)}\int u_\perp^2\,p\,J_n^2\,(\alpha^*\,u_\perp)\,e^{-u_\perp^2}\,u_\perp\,du_\perp$$

$$\bar{v}_{Di} = \frac{1}{\Gamma(p+1)}\iint\left\{\,2\omega\,(p+u_\perp^2) - \alpha^*\,\varepsilon a_i^*\,\Omega_i\,u_\perp^2\,\right\}$$

$$u_\perp^{2(p-1)}\,e^{-(u_\perp^2+u_\parallel^2)}\,J_n^2\,(\alpha^*\,u_\perp)\,\frac{\frac{1}{2}(u_\perp^2\,v_{\perp o}^2 + 2u_\parallel^2\,v_{\parallel o}^2)}{R_C\,\Omega_i}\,u_\perp\,du_\perp\,du_\parallel$$

$$a_i^* = \frac{v_{\perp o}}{\Omega_i} . \qquad \ldots (10)$$

Putting

$$\omega_D = \frac{-\,\omega_{pe}^2\,(\varepsilon - \frac{2}{R_C})}{k\,|\Omega_e|\,(1 + \frac{\omega_{pe}^2}{\Omega_e^2})}$$

and

$$\beta^2 = \frac{\omega_{pe}^2\,[\,2A(n\Omega_i - k_y\,\bar{v}_{Di}) - \alpha^*\,\varepsilon a_i^*\,\Omega_i\,B]\,\omega_D}{k_y^2\,v_{\perp o}^2\,(1 + \frac{\omega_{pe}^2}{\Omega_e^2})}$$

and solving equation (9), we obtain

$$\omega \approx \frac{n\Omega_i - k_y\,\bar{v}_{Di} + \omega_D}{2} \pm \left[\,\tfrac{1}{4}\left\{\,n\Omega_i - k_y\,v_{Di} + \omega_D(1 + \frac{B^2}{\omega_D^2})\,\right\}^2 - (n\Omega_i - k_y\,v_{Di})\,\omega_D\,\right]^{\frac{1}{2}} \qquad \ldots (11)$$

For instability, the following two inequalities must be satisfied:

$$\beta^2 > 0 \qquad \ldots (12)$$

and

$$\left(n\Omega_i - k_y \bar{v}_{Di} \right)\left(1 - \frac{2B}{\omega_D} \right) < \omega_D < \left(n\Omega_i - k_y \bar{v}_{Di} \right)\left(1 + \frac{2B}{\omega_D} \right) . \qquad \ldots (13)$$

Condition (13) is easily satisfied by choosing a suitable wavelength and a sufficiently high density. Hence the question of instability depends essentially on condition (12). Choosing $\omega_D = n\Omega_i - k_y \bar{v}_{Di}$ (and hence satisfying (13)) we may write inequality (12), the condition for instability, in the form

$$2A\omega_D + \alpha^* (-\varepsilon a_i^*) \Omega_i B > 0 . \qquad \ldots (14)$$

The quantities ω_D, α^*, $(-\varepsilon a_i^*)$, Ω_i and B are all positive and the sign of A depends upon the sign of p in the ion distribution function. In Appendix A, we show that for the loss-cone type of distribution there are always values of α^* giving $A > 0$. However if $p = 0$, one can show that A is always negative whatever the value of α^*.

Thus for loss-cone types of distributions ($p > 0$), inequality (14) may always be satisfied for some value of α^*. As mentioned earlier, the case of $p = 0$ (Maxwellian distribution) was discussed by Krall and Fowler[4], and these authors show that for suitable choices of electron and ion temperature and magnetic field curvature, one can keep the left hand side of inequality (14) negative for all values of α^*. So although one may completely stabilize the drift cyclotron instability with a Maxwellian distribution by magnetic field curvature, this is not the case for a loss-cone type of distribution. The growth rate for a loss-cone type distribution is found to be proportional to $(-\varepsilon + \frac{2}{R_C})^{\frac{1}{2}}$. Hence for magnetic well geometry, in which

$\varepsilon < 0$ and $R_C > 0$, the growth rate of the instability is increased compared with the uniform field case and the density threshold of the instability is correspondingly lowered.

To check the above analytical results, the complete dispersion equation (6) was computed for the loss-cone type of distribution with parameters of the PHOENIX II and ALICE mirror machines. In Figs.4 and 5 $\mathrm{Re}\,\frac{\omega}{\Omega_i}$ and $\mathrm{Im}\,\frac{\omega}{\Omega_i}$ are plotted as a function of α^*. It is seen that the magnetic well type of field curvature is slightly destabilizing and the range of unstable values of α^* is increased.

It is therefore concluded that it is impossible to stabilize the drift loss-cone cyclotron instability by field curvature in a minimum B type mirror machine.

4. EFFECT OF THE FINITE PLASMA SIZE

The model used in this section is again that of a plasma slab in a uniform magnetic field, but in this case the problem is solved properly without resorting to a local approximation and taking into account the appropriate boundary conditions. The wave again propagates in the y-direction with a wave vector k_y, while due to the density gradient in the x-direction the perturbed potential has to be of the form: $\varphi = \varphi(x)e^{ik_y y}$. The finite extent of the plasma in the x direction can be expected to introduce a 'radial' wave number k_x. In the plane wave local approximation, this would result in an effective gradient $\varepsilon_{eff} = \frac{k_y}{\sqrt{k_x^2 + k_y^2}}\,\varepsilon$ therefore the plasma is expected to be most unstable for small k_x. This problem of the finite plasma size was first considered by Shima and Fowler[5] in cylindrical geometry, who found analytically that, for a particular loss-cone distribution,

the radial potential distribution may be approximated by a slowly varying Bessel function, in agreement with what was expected. We develop here a method for calculating the potential wave forms, frequencies and critical densities for an arbitrary velocity distribution by solving a differential equation for $\varphi(x)$ subject to appropriate boundary conditions. This equation was obtained by expanding $\varphi(x)$ in the small parameter $(x' - x)$ prior to solving the Vlasov equation by orbit integration. In this expansion only the terms up to the second order in $(x' - x)$ were retained which resulted in a second order differential equation for $\varphi(x)$. This equation can be put into the form

$$\frac{\partial}{\partial\chi}\left[\mathcal{H}(\chi)\frac{\partial\varphi}{\partial\chi}\right] + c(\chi)\varphi = 0 \qquad \ldots (15)$$

where

$$\chi = \frac{x}{a_i} \quad , \quad \mathcal{H}(\chi) = a + b\chi \quad , \quad c(\chi) = d + e\chi$$

$$a = 1 - D\Omega S_1 + \frac{D\varepsilon a_i\,\Omega}{\alpha} S_2 + D\varepsilon a_i S_3$$

$$b = - D\varepsilon a_i\,\Omega\, S_1$$

$$d = - \alpha^2 + (D - \frac{D\varepsilon a_i\,\Omega}{\alpha}) F_1 + D\varepsilon a_i\,\alpha\, F_2 - \frac{D\alpha\varepsilon a_i}{\Omega}$$

$$e = D\varepsilon a_i F_1$$

and

$$S_1 = \frac{K_0}{\Omega(\Omega^2-1)} + \sum_{n=1}^{\infty}\left(\frac{\Omega-1}{(\Omega+n-1)(\Omega-n-1)} + \frac{\Omega+1}{(\Omega+n+1)(\Omega-n+1)} - \frac{2\Omega}{\Omega^2-n^2}\right) K_n$$

$$S_2 = \frac{K_0}{\Omega^2-1} + \sum_{n=1}^{\infty}\left(\frac{n^2+\Omega-1}{(\Omega+n-1)(\Omega-n-1)} + \frac{n^2-\Omega-1}{(\Omega+n+1)(\Omega-n+1)} - \frac{2n^2}{\Omega^2-n^2}\right) K_n$$

$$+ \sum_{n=1}^{\infty}\frac{1}{2\alpha^2}\left(\frac{\Omega(1-2n)}{(\Omega+n)(\Omega-n+1)} - \frac{\Omega(1-2n)}{(\Omega-n)(\Omega+n-1)}\right) I_{n-1,n}$$

$$S_3 = \sum_{n=1}^{\infty}\left(\frac{1-2n}{(\Omega+n-1)(\Omega-n)} - \frac{1-2n}{(\Omega+n)(\Omega-n+1)}\right) W_{n-1,n} \quad .$$

Here the integrals $I_{n-1,n}$, K_o, and K_n have already been defined in Section 2 and the additional integral $W_{n-1,n}$ is given by

$$W_{n-1,n} = \int \Psi(y^2)\, y^2\, J_n(\alpha y)\, J_{n-1}(\alpha y)\, dy$$

Equation (15) was solved numerically for the boundary conditions

$$\varphi(0) = 0$$

and

$$\frac{\left[\frac{d\varphi(\chi)}{d\chi}\right]_{\chi = \chi_o}}{\varphi(\chi_o)} = \frac{-k_y}{\mathcal{H}(\chi_o)}$$

where χ_o is the width of the plasma slab. The latter condition was obtained by integrating the equation (15) across the boundary. The numerical procedure for finding the roots Ω_ℓ consisted of starting off from the point $\chi = \chi_o$ with the slope satisfying the boundary condition and then following the solution to $\chi = 0$. The frequency $\Omega = \omega/\Omega_i$ was then treated as a parameter and varied in small steps until a solution was found which satisfied the condition $\varphi(0) = 0$. Several radial modes were found at each normalised density, for a fixed k_y, and they are shown in Figs.6 and 7. The normalised density $D = \frac{\omega_{pi}^2}{\Omega_i^2}$ is then plotted as a function of the roots Ω_ℓ in Fig.8 for $\varepsilon = -0{\cdot}1$ and a value of $\alpha = k_y a_i = 3{\cdot}5$ known to be the most unstable from the local approximation. The range of Ω was limited to the most unstable region $0 < \Omega < 1$. The critical values of D can be obtained from Fig.8 in the usual way as the maximum of the curves $D(\Omega_\ell)$ versus Ω_ℓ. It is seen that the solutions for $\ell = 0$, where ℓ is the radial mode number, are only marginally more stable than the local solution for the point of maximum density in the plasma slab.

5. CONCLUSION

The ion cyclotron drift loss-cone instability is found to be unstable for steep particle density gradients. The high density stable regimes for steep electron density gradients are removed when the equally steep ion density gradient is taken into consideration.

Magnetic well type of field curvature is found to be slightly destabilizing (i.e. the density thresholds for instability are lowered) for loss-cone type of velocity distributions in contrast to the results for the near-Maxwellian type of distribution.

The density thresholds for instability derived by using the local approximation differ only slightly from the instability thresholds found for the boundary value problem, provided the local approximation is applied to the point of maximum density.

ACKNOWLEDGEMENTS

We would like to thank most warmly C.A. Steed for his efficiency and enthusiasm in the arduous task of computing these results. We are also grateful to F.M. Larkin and P. Keeping for discussions on numerical methods. We also express our gratitude to Dr P.C.Thonemann for his encouragement throughout the work and for helpful comments.

REFERENCES

1. MIKHAILOVSKII, A.B. and TIMOFEEV, A.V., Zh. Eksperim. i Teor. Fiz. 44, 919 (1963) [English transl.: Soviet Phys. - JETP 17, 626 (1963)].

2. POST, R.F. and ROSENBLUTH, M.N., Phys. Fluids 9, 730 (1966).

3. POST, R.F., Lawrence Radiation Laboratory Annual Report July 1965-June 1966, UCRL-50002-66-1 p.53-57.

4. KRALL, N.A. and FOWLER, T.K., Phys. Fluids 10, 1526 (1967).

5. SHIMA, Y. and FOWLER, T.K., Phys. Fluids 8, 2245 (1965).

6. As the theory is only applicable in the case where $|\varepsilon a_i| \ll 1$ the use of $\varepsilon a_i = -0{\cdot}8$ may be considered to be suspect; although the results still are qualitatively correct.

APPENDIX A

We show that $A > 0$ for $p > 0$ and $n \geqslant 1$. From equation (10) we may write A in the form

$$A = \int_0^\infty \frac{\partial}{\partial u_\perp^2}(u_\perp^{2p}\, e^{-u_\perp^2})\, J_n^2(\alpha^* u_\perp)\, du_\perp^2 \quad .$$

Integration by parts gives

$$A = -\frac{\alpha^*}{2}\frac{\partial}{\partial \alpha^*}\, R_p(\alpha^*)$$

where

$$R_p(\alpha^*) = \int_0^\infty u_\perp^{2(p-1)}\, e^{-u_\perp^2}\, J_n^2(\alpha^* u_\perp)\, du_\perp^2 \quad .$$

Thus for $A > 0$ we require the slope of $R_p(\alpha^*)$ to be negative for some α^*.

Now $R_p(0) = 0$ for all p provided $n > 0$, and it is easily shown that $R_p(\alpha^*) \to 0$ as $\alpha^* \to \infty$ for $p > 0$. Since $R_p(\alpha^*)$ is continuous and positive in the region $0 < \alpha^* < \infty$ then the slope of $R_p(\alpha^*)$ must be negative for some α^* in this region. Hence $A > 0$ provided $p > 0$ and $n > 0$.

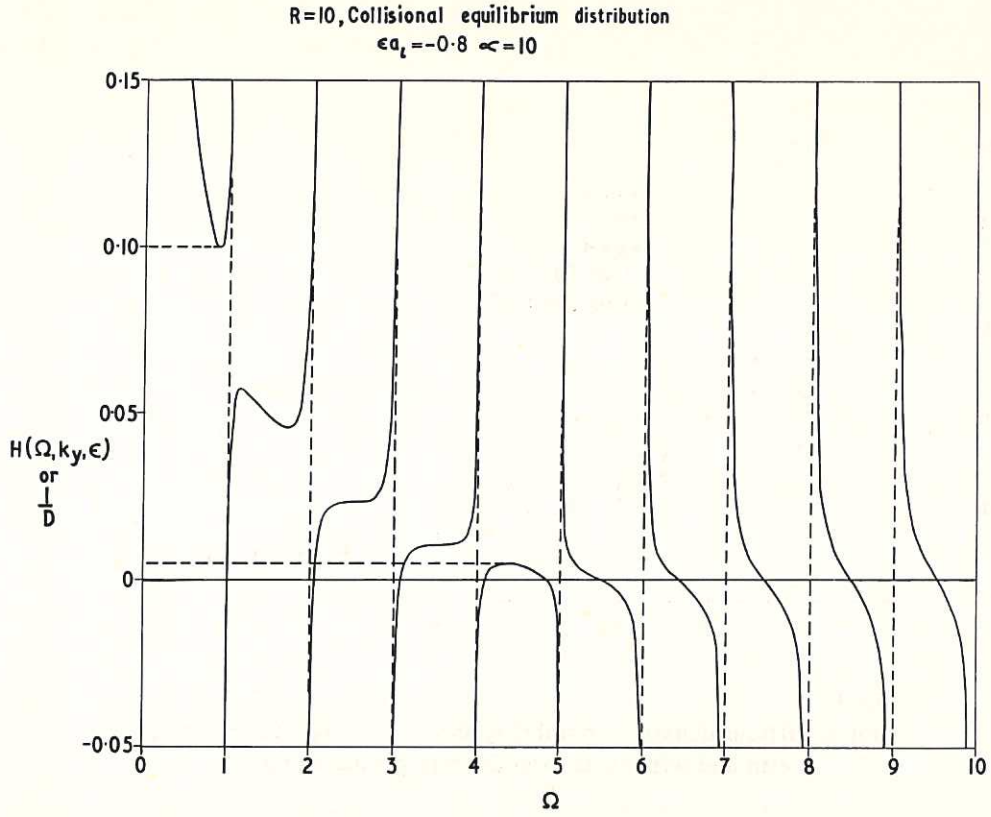

Fig. 1 (CLM-P 157)

Plot of $H(\Omega, k_y, \epsilon)$ against Ω from the dispersion equation (5A) which does not contain the ion density gradient term.

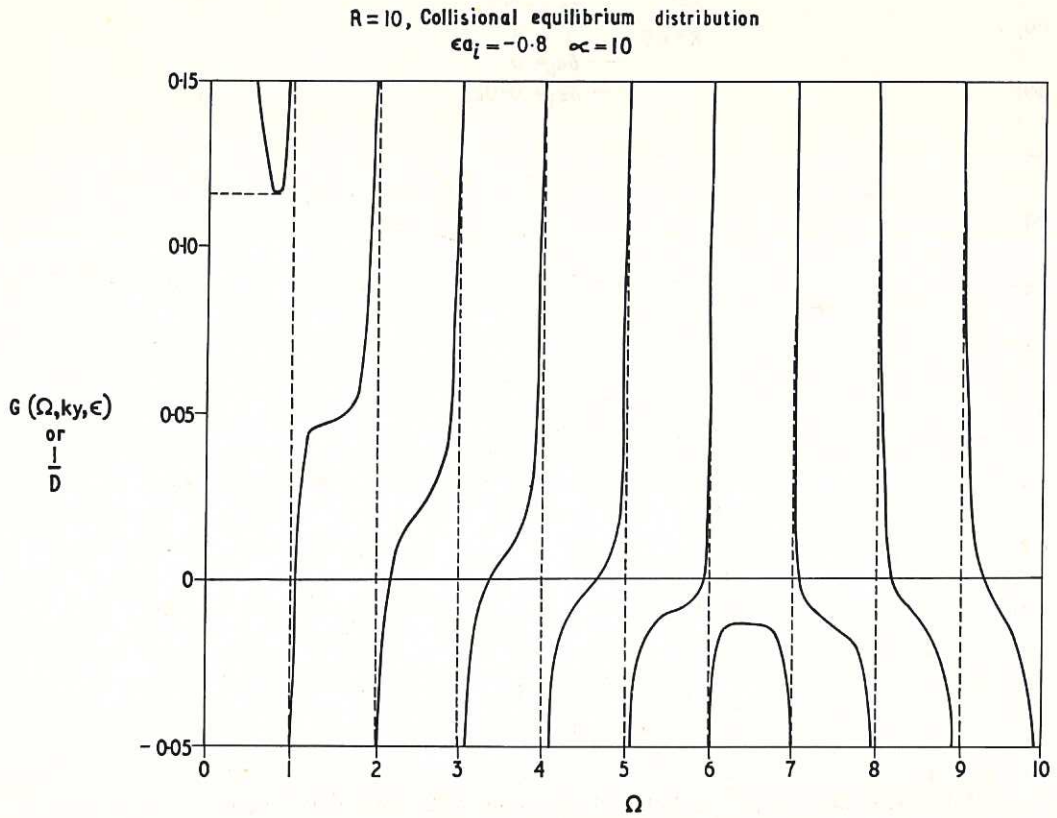

Fig. 2 (CLM-P 157)

Plot of $G(\Omega, k_y, \epsilon)$ against Ω from the dispersion equation (5) which contains the ion density gradient term.

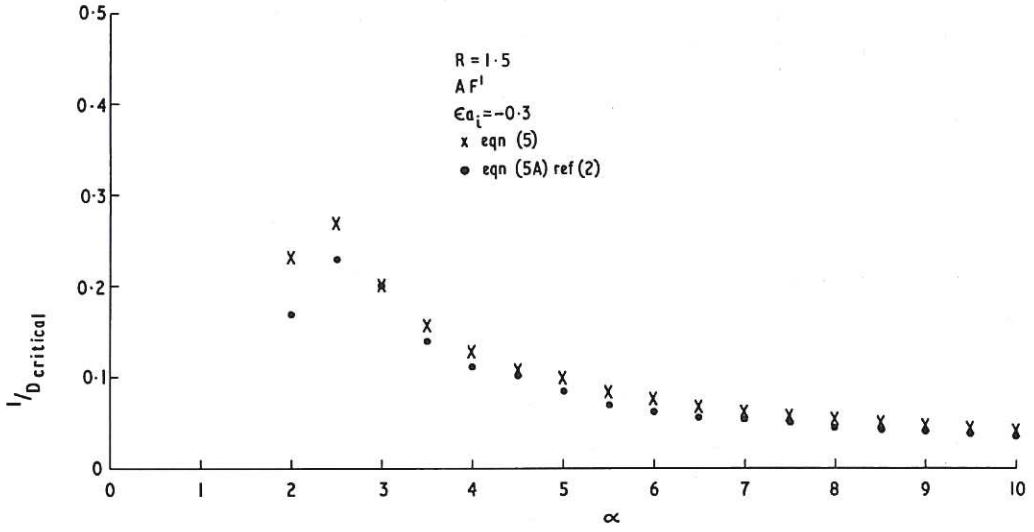

Fig. 3 (CLM-P 157)
Plot of critical density - instability threshold - against $\alpha = k_y a_i$ with and without the ion density gradient term.

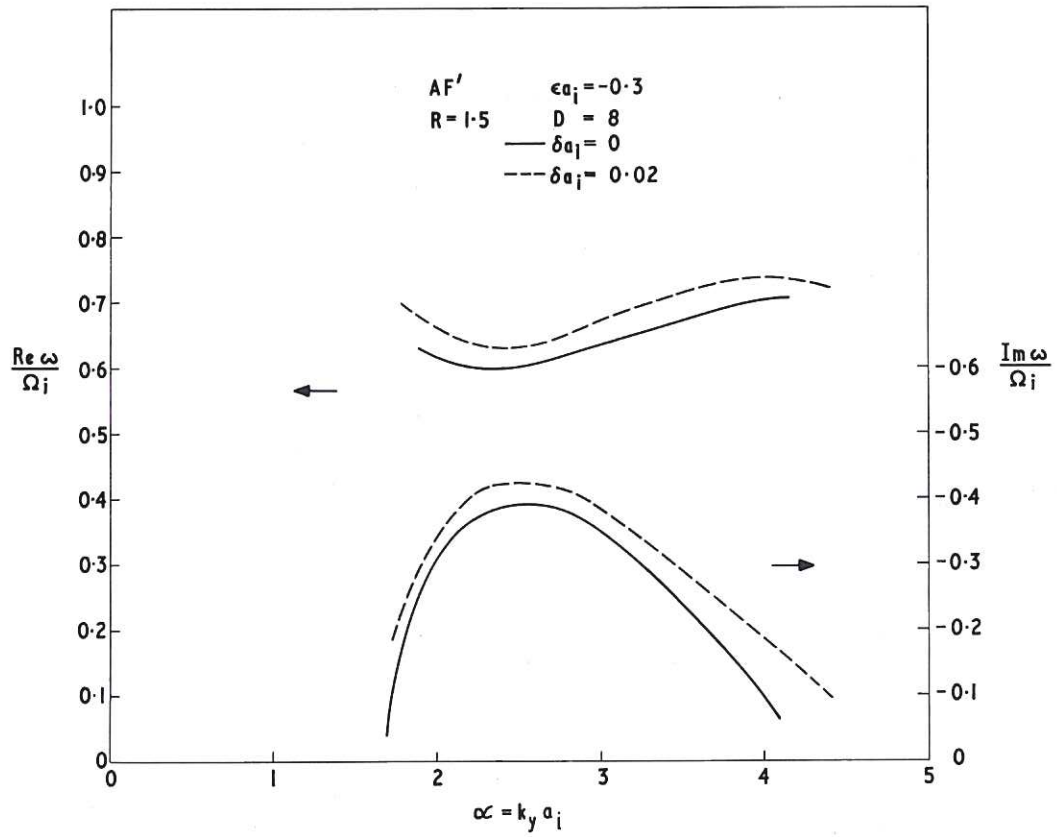

Fig. 4 (CLM-P 157)
Plot of real and imaginary parts of the frequency against $\alpha = k_y a_i$ for typical PHOENIX II parameters.

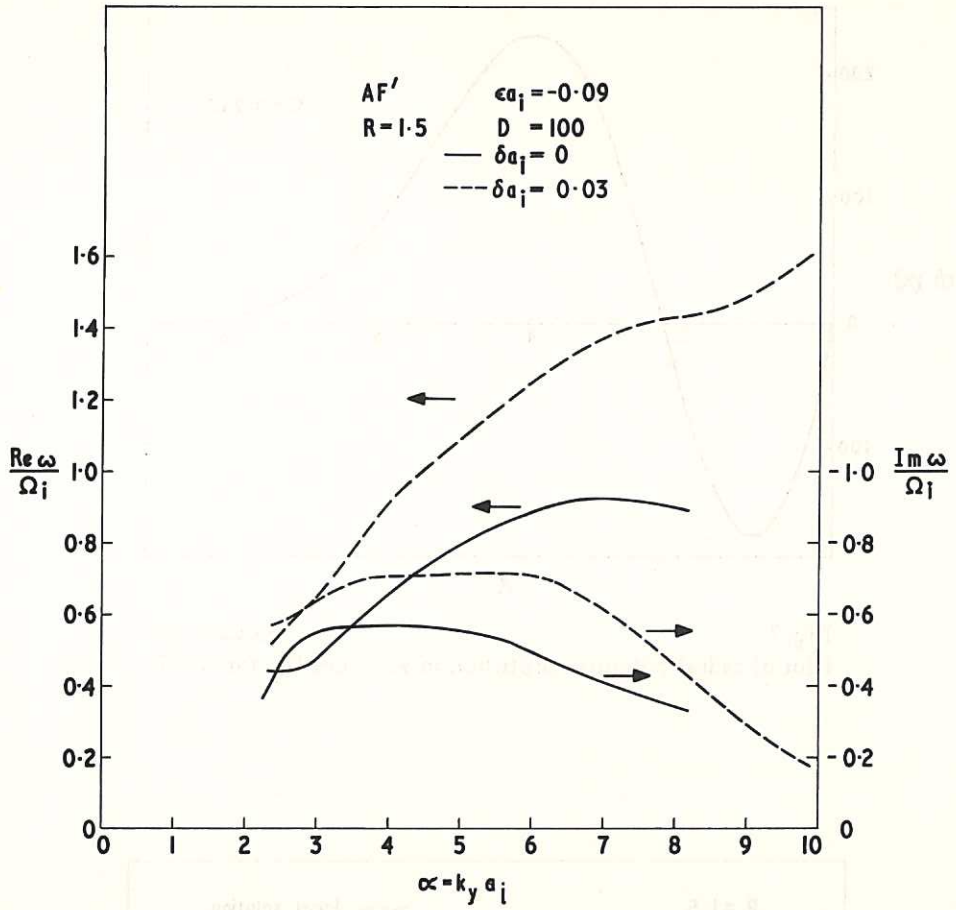

Fig. 5 (CLM-P 157)

Plot of real and imaginary parts of the frequency against $\alpha = k_y a_i$ for typical ALICE parameters.

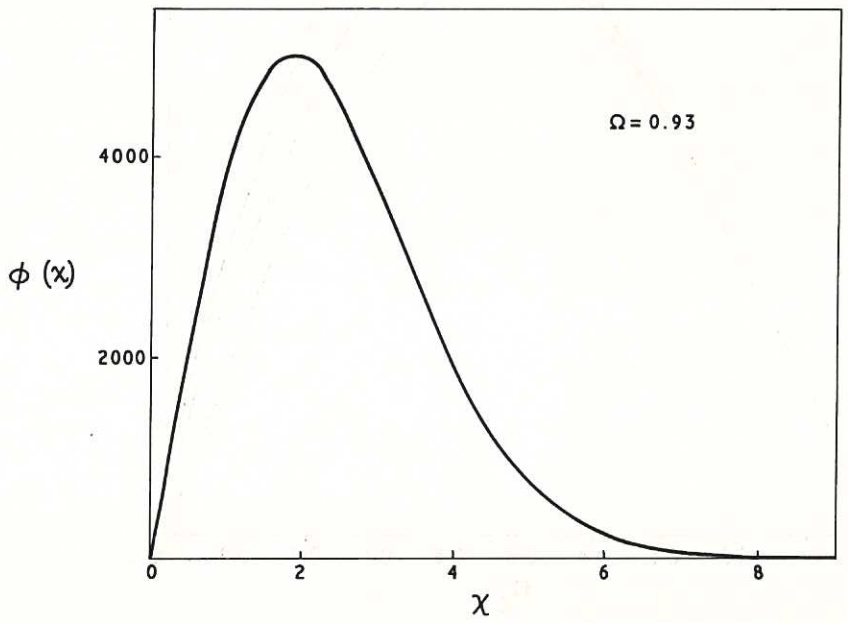

Fig. 6 (CLM-P 157)

Plot of radial potential distribution at a root Ω_ℓ for $\ell = 0$.

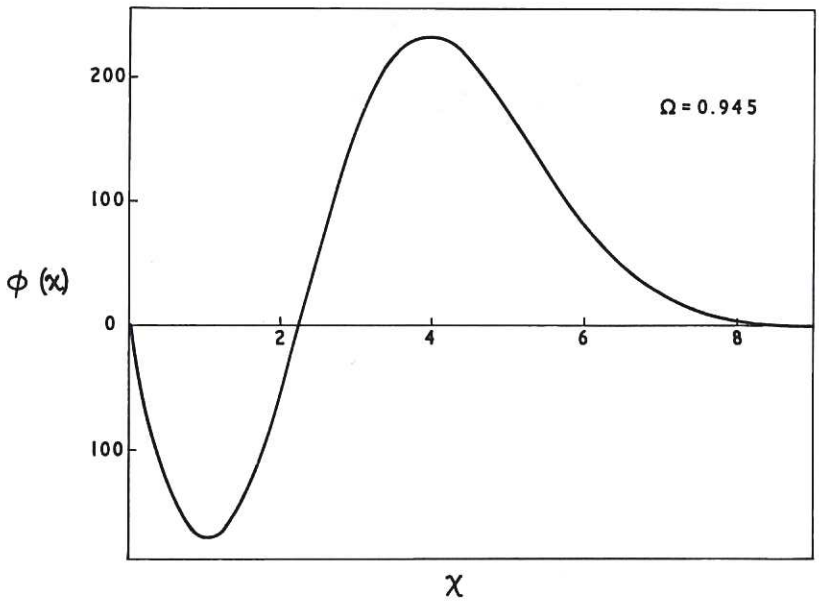

Fig. 7 (CLM-P 157)
Plot of radial potential distribution at a root Ω_ℓ for $\ell = 1$.

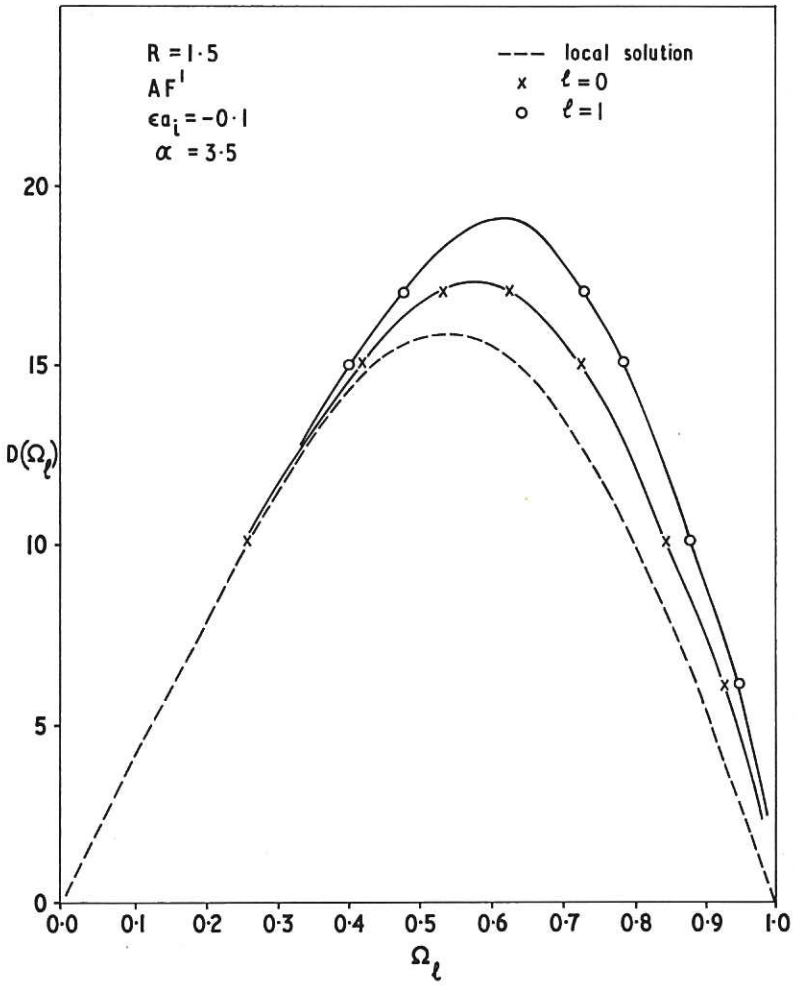

Fig. 8 (CLM-P 157)
Plot of density against Ω_ℓ for the result from local approximation and for $\ell = 0, 1$.